Effects of electric and magnetic fields on confined donor states in a dielectric quantum well

J. Cen and K. K. Bajaj
Department of Physics, Emory University, Atlanta, Georgia 30322
(Received 23 April 1993)

We have developed a variational formalism for the calculation of the binding energies of hydrogenic donors in the so-called "dielectric quantum wells," where the dielectric constant of the barrier material is significantly smaller than that of the well material, in the presence of magnetic and electric fields applied along the growth axis. We derive an expression for the anisotropic electron–donor-ion interaction potential analytically by solving the Poisson equation in the layered geometry of quantum-well structures. Binding energies of the $1s$ and $2p$ states are then calculated using the Gaussian-type orbital expansion method. Effects of the applied electric field, magnetic field, and the interfacial dielectric-constant mismatch on the binding energies of donor states are studied in detail.

INTRODUCTION

Dielectric quantum wells have recently received increasing attention because of progress in fabrication processes and their potential to sustain electro-optic operations with a greater range of applicable electric fields.[1–6] The enhancement of the Coulomb interaction in a thin semiconductor layer sandwiched between insulators was first pointed out by Keldysh in 1979.[1] A quantum well can be called "dielectric" when the dielectric constant of the barrier material is significantly smaller than that of the well material, as in the case of a GaAs-ZnSe quantum well and other structures constructed according to the same principle.[7–10] Image charges arise due to the mismatch of dielectric constants at the interfaces. Binding energies of donors can be significantly enhanced because of the additional confinement effect produced by the image charge distribution, which may also provide the interesting possibility of constructing devices at desired wavelengths using transitions among states associated with different electronic subbands with appropriate choices of material parameters such as dielectric constants and conduction-band mismatch.

While many groups have studied impurity states in nondielectric quantum-well structures[11–33] there is also a need to study donor states in the dielectric quantum-well structures, where the effects of applied electric and magnetic fields are also dependent on the dielectric environment. Calculations of the binding energies and their variations with the applied fields are needed to obtain accurate values of the optical transition energies of donors and excitons in such quantum wells.

In this paper, we report our calculation of the donor binding energies in the dielectric quantum wells, in the presence of parallel electric and magnetic fields applied along the growth direction. We calculate the variations of the binding energy of the $1s$ state, and the $1s \rightarrow 2p_+$ transition energy, as a function of the applied electric and magnetic fields, with various choices of the dielectric constants, and discuss how the electric- and magnetic-fields effects on the donor states depend on the dielectric confinement.

FORMALISM

We consider a dielectric quantum well depicted in Fig. 1, with the electric and magnetic fields **E** and **B** applied parallel to the growth axis (chosen as the z direction). The width of the quantum well is L. The origin is chosen such that $z=\pm L/2$ marks the right (left) boundary of the well. The dielectric constant in the well is ε_1, and that in the barrier is ε_2 ($\varepsilon_2<\varepsilon_1$). The location of a donor ion in the quantum well is denoted as $(0,0,z_0)$. Because of the difference in the dielectric constants, an electron not only sees the donor ion itself, but also the image charge distribution. In what follows, instead of tediously finding the positions of the image charges and the corresponding potential, we solve the first-principle Poisson equation in the layered quantum-well geometry to obtain the expression of the potential between the electron and the image charge distribution. The potential $\Phi(\mathbf{r})$ produced by a unit charge at $z=z_0$ satisfies

$$\varepsilon\nabla^2\Phi(\mathbf{r})=-4\pi\delta(z-z_0)\ , \tag{1}$$

the solution of which in the cylindrical coordinates is independent of the azimuthal angle φ. We therefore can write $\Phi(\mathbf{r})$ in the general form[34]

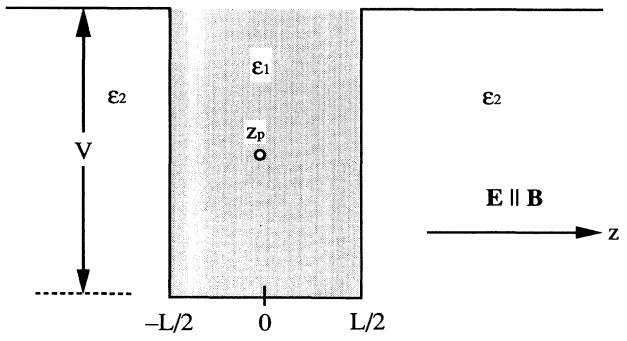

FIG. 1. Schematic conduction-band diagram for a dielectric quantum-well structure. The electric field **E** and magnetic field **B** are applied parallel to the growth direction of the structure.

$$\Phi(\mathbf{r})=\int_0^\infty d\kappa\, f(\kappa,z)J_0(\kappa\rho)\ , \tag{2}$$

where $\rho=\sqrt{x^2+y^2}$ and $J_0(\kappa\rho)$ is the Bessel function of the zeroth order, $f(\kappa,z)$ is a function to be determined from boundary conditions on $\Phi(\mathbf{r})$, i.e., $\Phi(\mathbf{r})$, and $\varepsilon_i\partial\Phi_i(\mathbf{r})/\partial z$ $(i=1,2)$ is continuous across the interfaces. Since $\Phi(\mathbf{r})$ is uniquely determined by the function $f(\kappa,z)$, we now proceed to obtain its expression.

For a donor located within the quantum well ($|z_0|<L/2$), $f(\kappa,z)$ in the quantum well and the barrier regions can be written as[34]

$$f_1(\kappa,z)=e^{-\kappa|z-z_0|}+Ae^{-\kappa z}+Be^{\kappa z} \quad (|z|<L/2\ ,\ \text{region 1})\ , \tag{3a}$$

$$f_2(\kappa,z)=Ce^{-\kappa z} \quad (z>L/2\ ,\ \text{region 2})\ , \tag{3b}$$

$$f_3(\kappa,z)=De^{\kappa z} \quad (z<-L/2\ ,\ \text{region 3})\ , \tag{3c}$$

where the first term in $f_1(\kappa,z)$ is the contribution from the unit charge itself, and A, B, C, and D are constants to be determined. At $z=L/2>z_0$,

$$f_1=f_2\ ,\quad \varepsilon_1\frac{\partial f_1}{\partial z}=\varepsilon_2\frac{\partial f_2}{\partial z}\ , \tag{4a}$$

and at $z=-L/2<z_0$,

$$f_3=f_1\ ,\quad \varepsilon_2\frac{\partial f_3}{\partial z}=\varepsilon_1\frac{\partial f_1}{\partial z}\ , \tag{4b}$$

which leads to a set of linear equations

$$A+Be^{\kappa L}-C=-e^{\kappa z_0}\ , \tag{5a}$$

$$A-Be^{\kappa L}-C\bar{\varepsilon}=-e^{\kappa z_0}\ , \tag{5b}$$

$$Ae^{\kappa L}+B-D=-e^{-\kappa z_0}\ , \tag{5c}$$

$$Ae^{\kappa L}-B+D\bar{\varepsilon}=e^{-\kappa z_0}\ , \tag{5d}$$

where $\bar{\varepsilon}=\varepsilon_2/\varepsilon_1<1$. We obtain the following expression of the electron–donor-ion effective Coulomb interaction after substituting the solutions of the above equations into Eqs. (3) and (2) (in units of the effective Rydberg, defined later in this section):

$$H_c=-2\int_0^\infty d\kappa\, v(z,z_0;\kappa)J_0(\kappa\rho)\ , \tag{6}$$

in which

$$v(z,z_0;\kappa)=\begin{cases}\dfrac{2}{(1+\bar{\varepsilon})}\dfrac{e^{-\kappa z+(\kappa L+\eta)/2}\cosh[\kappa z_0+(\kappa L+\eta)/2]}{\sinh(\kappa L+\eta)}\ , & z\geq\dfrac{L}{2}\\[2ex] \dfrac{2\cosh[\kappa z_>-(\kappa L+\eta)/2]\cosh[\kappa z_<+(\kappa L+\eta)/2]}{\sinh(\kappa L+\eta)}\ , & |z|\leq\dfrac{L}{2}\\[2ex] \dfrac{2}{(1+\bar{\varepsilon})}\dfrac{e^{\kappa z+(\kappa L+\eta)/2}\cosh[\kappa z_0-(\kappa L+\eta)/2]}{\sinh(\kappa L+\eta)}\ , & z\leq-\dfrac{L}{2}\ ,\end{cases} \tag{7}$$

where $\eta=\ln[(1+\bar{\varepsilon})/(1-\bar{\varepsilon})]$, $z_>=\max(z,z_0)$, and $z_<=\min(z,z_0)$. Expressions for which the donor is located outside the quantum well can be obtained in a similar fashion. It is easy to see that if the dielectric constants were the same across the interfaces, then $\eta\to\infty$ and $v(z,z_0;\kappa)\to e^{-\kappa|z-z_0|}$. One recovers the usual expression for the Coulomb interaction $H_c=-2/r$.

Within the framework of an effective-mass approximation, the Hamiltonian of a donor in the quantum-well structure is written as

$$H=H_z+H_\parallel+H_c\ , \tag{8}$$

where all the lengths are scaled in terms of the effective Bohr radius $a_B=\varepsilon_1\hbar^2/\mu_1e^2$, and all energies in the effective Rydberg $R=e^2/2\varepsilon_1a_B$, μ_1 is the effective electron mass inside the quantum well, and

$$H_z=-\frac{\partial}{\partial z}\frac{\mu_1}{\mu_z}\frac{\partial}{\partial z}+V_{\rm QW}(z)+V_{\rm SE}(z)+\mathcal{E}z\ , \tag{9a}$$

$$H_\parallel=-\frac{\mu_1}{\mu_z}\left[\frac{1}{\rho}\frac{\partial}{\partial\rho}\rho\frac{\partial}{\partial\rho}+\frac{1}{\rho^2}\frac{\partial^2}{\partial\varphi^2}\right]+\frac{\mu_1}{\mu_z}\left[\gamma L_z+\frac{\gamma^2\rho^2}{4}\right]\ , \tag{9b}$$

where μ_z is the material-dependent effective electron mass, $V_{\rm QW}(z)$ is the potential profile of the quantum-well structure, and

$$V_{\rm SE}(z)=\int_0^\infty\frac{d\kappa}{\sinh(\kappa L+\eta)}\times\begin{cases}-\dfrac{\sinh\kappa L}{\bar{\varepsilon}}e^{\kappa(L-2|z|)}\ , & |z|>\dfrac{L}{2}\\[2ex] \cosh2\kappa z+e^{-\kappa L-\eta}\ , & |z|\leq\dfrac{L}{2}\end{cases} \tag{10}$$

is the self-polarization energy from the interaction between the electron and its image charge distribution; $\mathcal{E}=e|\mathbf{E}|a_B/R$ is the strength of the applied electric field, $\gamma=e\hbar B/2\mu_1 cR$ is energy of the first Landau level, L_z is the z component of the angular momentum (in units of $\hbar$), and H_c is the term describing the effective anisotropic Coulomb attraction between the electron and the donor ion defined in Eq. (7).

Instead of solving for the exact subband wave functions in the absence of the Coulomb attraction, we treat the $\mathcal{E}z$, $H_{\|}$, and H_c terms in the Hamiltonian variationally and proceed to determine the energy levels and wave functions in a two-step procedure. Such an approximation simplifies the formalism without losing much validity if the electric field is not too strong as to eject the electron from the bound state.[35] For the wave function $F_k(z)$ along the growth direction, we solve the Schrödinger equation $H_z F_k(z)=E_k F_k(z)$ where E_k is the kth subband energy. It has been shown[36] that the effect of the self-polarization energy can be satisfactorily accounted for by a shift in the subband energy, without significant modification of the subband wave function. Since such shifts are canceled out in the results for the binding energies and transition energies, $V_{\rm SE}(z)$ will be dropped from the Hamiltonian in the rest of this paper. First we solve for the subband wave function $F_k^0(z)$ in the absence of the electric field by writing $F_k^0(z)$ in the following form:[37]

$$F_k^0(z)=\begin{cases} A_k\cos[\omega_k z-(k-1)\pi/2], & |z|<L/2 \\ D_k\exp[-\sigma_k(z-L/2)], & z>L/2 \\ (-1)^{k-1}D_k\exp[\sigma_k(z+L/2)], & z<-L/2 \end{cases} \tag{11}$$

and requiring that $F_k^0(z)$ and $\mu_z^{-1}\partial F_k^0(k)/\partial z$ be continuous across the interfaces at $z=\pm L/2$ to obtain the secular equation

$$\cos[\omega_k L/2-(k-1)\pi/2] - \frac{\mu_2\omega_k}{\mu_1\sigma_k}\sin[\omega_k L/2-(k-1)\pi/2]=0 , \tag{12}$$

for the subband level $E_k^0=\omega_k^2$, where $\sigma_k=\sqrt{\mu_2(V-E_k^0)/\mu_1}$, μ_2 is the effective mass in the barrier material. We then assume that the wave function is modified by the electric field as follows:[38]

$$F_k^0(z)\rightarrow F_k(z)=\exp(-\lambda_k z)F_k^0(z) \quad (\mathcal{E}\lambda_k\geq 0) ,$$

to account for the redistribution of the electronic charge density under an electric field, and that the energy level E_k is determined from minimization of the following expression with respect to λ_k:

$$\langle E_k(\lambda_k)\rangle=\frac{\langle F_k|H_z|F_k\rangle}{\langle F_k|F_k\rangle}=\frac{E_k^0 M_1+\lambda_k^2 M_2+\mathcal{E}N_1}{M_1} , \tag{13}$$

where

$$M_1=\int_{-\infty}^{\infty}dz|F_z^0(z)|^2\exp(-2\lambda_k z)$$
$$=\frac{A_k^2}{2}\left[\frac{\sinh\lambda_k L}{\lambda_k}-(-1)^k\frac{\omega_k\sin\omega_k L\cosh\lambda_k L+\lambda_k\cos\omega_k L\sinh\lambda_k L}{\omega_k^2+\lambda_k^2}\right]+\frac{D_k^2}{2}\left[\frac{e^{-\lambda_k L}}{\sigma_k+\lambda_k}+\frac{e^{\lambda_k L}}{\sigma_k-\lambda_k}\right] , \tag{14a}$$

$$M_2=\int_{-\infty}^{\infty}dz\frac{\mu_1}{\mu_2}|F_k^0(z)|^2\exp(-2\lambda_k z)$$
$$=\frac{A_k^2}{2}\left[\frac{\sinh\lambda_k L}{\lambda_k}-(-1)^k\frac{\omega_k\sin\omega_k L\cosh\lambda_k L+\lambda_k\cos\omega_k L\sinh\lambda_k L}{\omega_k^2+\lambda_k^2}\right]+\frac{D_k^2}{2}\frac{\mu_1}{\mu_2}\left[\frac{e^{-\lambda_k L}}{\sigma_k+\lambda_k}+\frac{e^{\lambda_k L}}{\sigma_k-\lambda_k}\right] , \tag{14b}$$

$$N_1=\int_{-\infty}^{\infty}dz|F_k^0(z)|^2 z\exp(-2\lambda_k z)=-\frac{1}{2}\frac{\partial M_1}{\partial\lambda_k} . \tag{14c}$$

$\lambda_k^{\min}$ is then obtained as a solution of $\partial\langle E_k(\lambda_k)\rangle/\partial\lambda_k=0$,

$$\lambda_k^2(M_1M_2'-M_1'M_2)+2\lambda_k M_1M_2+\frac{\mathcal{E}}{2}[(M_1')^2-M_1M_1'']=0 , \tag{15}$$

where M' and M'' are the first and second derivatives of M with respect to λ_k.

We write the total wave function as follows:

$$\Psi(\mathbf{r})=\sum_{k=1}A_k F_k(z)\phi(\rho,\varphi;z-z_p) , \tag{16}$$

where $F_k(z)$ is the kth eigenfunction of H_z, and A_k is a measure of contribution to $\Psi(\mathbf{r})$ from the kth subband wave function. $\phi(\rho,\varphi;z)$, as a function describing the binding between the electron and the donor ion, is expressed as an expansion in Gaussian-type orbitals,[13,20]

$$\phi(\rho,\varphi;z)=\frac{e^{im\varphi}}{\sqrt{2\pi}}\rho^{|m|}e^{-\beta\rho^2}\sum_{i=1}c_i e^{-\alpha_i(\rho^2+z^2)} \quad (m=0,\pm1,\ldots) , \tag{17}$$

where β is a variational parameter, m is the azimuthal quantum number, and α_i are the Gaussian-type orbital expansion coefficients adopted from the variational results of Huzinaga.[39] A_k and c_i are the remaining expansion coefficients to be determined from the minimization of the total energy. The Schrödinger equation $H\Psi=E\Psi$ is then expressed as a generalized matrix equation,[33]

$$[H(kl;ij)-EU(kl;ij)]A_i c_j=0 , \tag{18}$$

and the total energy E is obtained as one of the eigenvalues, which is subsequently minimized with respect to the variational parameter β. Effects of electric and magnetic fields on excited states can be calculated in a similar fashion. The binding energies of the $1s$ ($m=0$) and $2p_{\pm}$ ($m=\pm 1$) donor states associated with the kth subband are defined as $E_B=E_k+(m+|m|+1)\gamma-E$; the $1s\rightarrow 2p_+$ transition energy is obtained as $E_T=E(2p_+)-E(1s)$.

RESULTS AND DISCUSSION

We have calculated the $1s$ donor binding energy in a GaAs-ZnSe dielectric quantum-well structure. First setting $B=0$ and $\varepsilon_2=\varepsilon_1$, and using the same material parameters as used in Ref. 19, we reproduce the results of Ref. 19 of the binding energy of the $1s$ donor state in a single quantum well under an applied electric field. The effective electron mass in GaAs is $\mu_1=0.067m_e$, and the dielectric constant is taken as $\varepsilon_1=12.5$. The effective Bohr radius $a_B=100$ Å; the effective Rydberg energy $R=5.8$ meV. $\gamma=1$ corresponds to $B=67$ kG, and $\mathcal{E}=1$ to $|\mathbf{E}|=5.8$ kV/cm. The material parameters of ZnSe are those used in Ref. 3, i.e., $\mu_2=0.17m_e$, $\varepsilon_2=7.6$. The potential barrier height in the GaAs-ZnSe structure is assumed to be $V=340$ meV. For the quantum-well structures considered here, separation in energy between neighboring subbands is larger compared to the expected donor binding energies. In this paper, we present only results for the $1s$ ($m=0$) binding energy and the $1s\rightarrow 2p_+$ ($m=1$) transition energy of donor states associated with the lowest electronic subband.

To see the effect of the dielectric confinement, we show in Fig. 2 the variation of the binding energies of a donor at the center of the dielectric quantum well as a function of the quantum-well size, in the absence of applied fields. Three cases are considered (represented by curves 1–3) to study the effects of the image charge distribution and dielectric screening. For curve 1, the actual dielectric constants are used; for curve 2, the average of the two dielectric constants is used for both the well and barrier

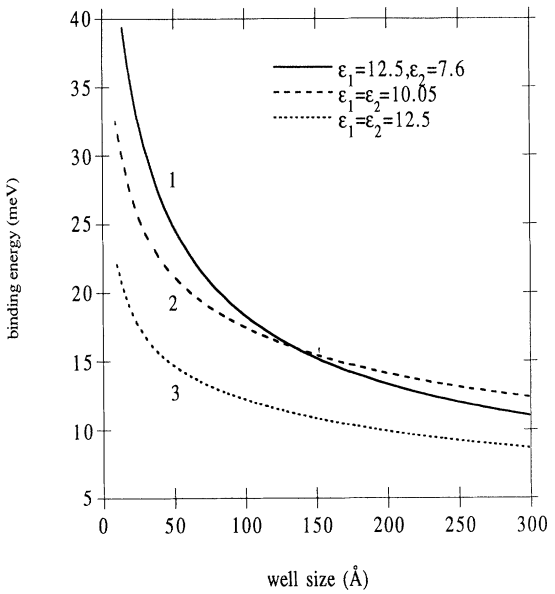

FIG. 2. Variation of the $1s$ binding energy of a well-center donor as a function of the well size, in GaAs-ZnSe quantum-well structures in the absence of applied fields. The dielectric constant of the well layer is ε_1, and that of the barrier material is ε_2. $\varepsilon_1=12.5$, $\varepsilon_2=7.6$ for curve 1 (solid line); $\varepsilon_1=\varepsilon_2=10.1$ for curve 2 (dashed line, $R=8.9$ meV); and $\varepsilon_1=\varepsilon_2=12.5$ for curve 3 (dotted line, $R=5.8$ meV).

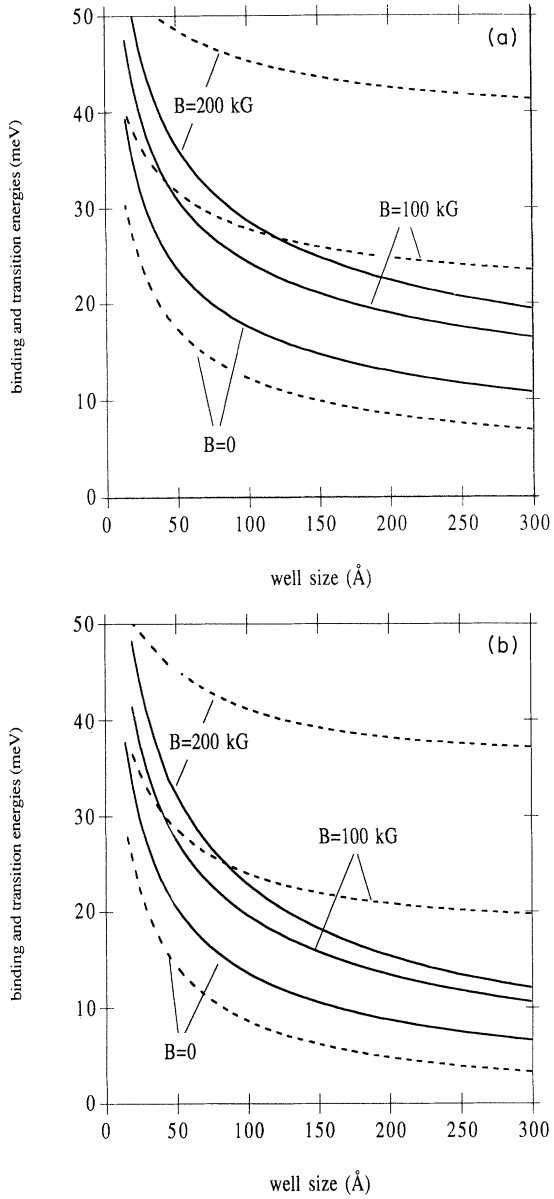

FIG. 3. Variations of the $1s$ binding energy (solid lines) and the $1s\rightarrow 2p_+$ transition energy (dashed lines) as functions of the well size, in GaAs-ZnSe quantum-well structures in a zero electric field, for a donor located at (a) the center of the well and (b) the edges of the well. The dielectric constant of the well layer is 12.5, and that of the barrier material is 7.6. Other parameters are noted in the text.

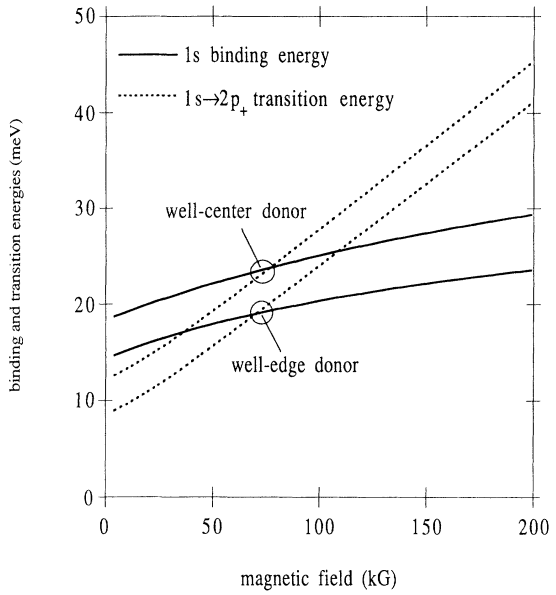

FIG. 4. Variations of the $1s$ donor binding energy and, the $1s \rightarrow 2p_+$ transition energy as functions of the applied magnetic field in a 100-Å GaAs-ZnSe dielectric quantum well, for donors located at the center and at the edges of the quantum well.

materials; for curve 3, the dielectric constant of the well layer is used in the calculation for both the well and barrier materials. It is obvious that ignoring the image charge by using the dielectric constant of the well material (as in curve 3) leads to consistently lower binding energies, even for wider quantum wells where only the long-range Coulomb interaction with the image charge distribution is ignored. In contrast, by using the average dielectric constant for the whole QW structure (as in curve 2), we effectively reduced the dielectric constant inside the quantum well, and increased that in the barriers. At large well sizes, the wave function is mainly inside the quantum well, the reduced screening implied by a smaller dielectric constant in the well region leads to larger binding energies than those in curve 1. In such cases, reduced screening more than compensated for the effect of the image charge distribution on the binding energies. At smaller well sizes, however, an increasing portion of the wave function is in the barrier region with the increased screening implied by a larger dielectric constant, so the

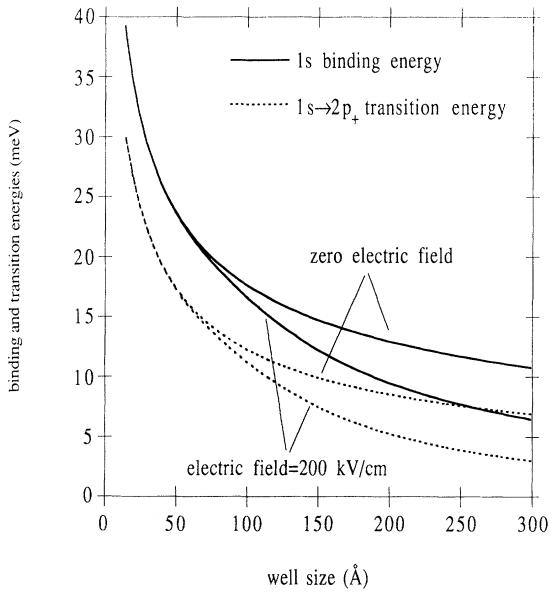

FIG. 5. Variation of the $1s$ donor binding energy as a function of the well size in a GaAs-ZnSe dielectric quantum well, in the presence of an applied electric field.

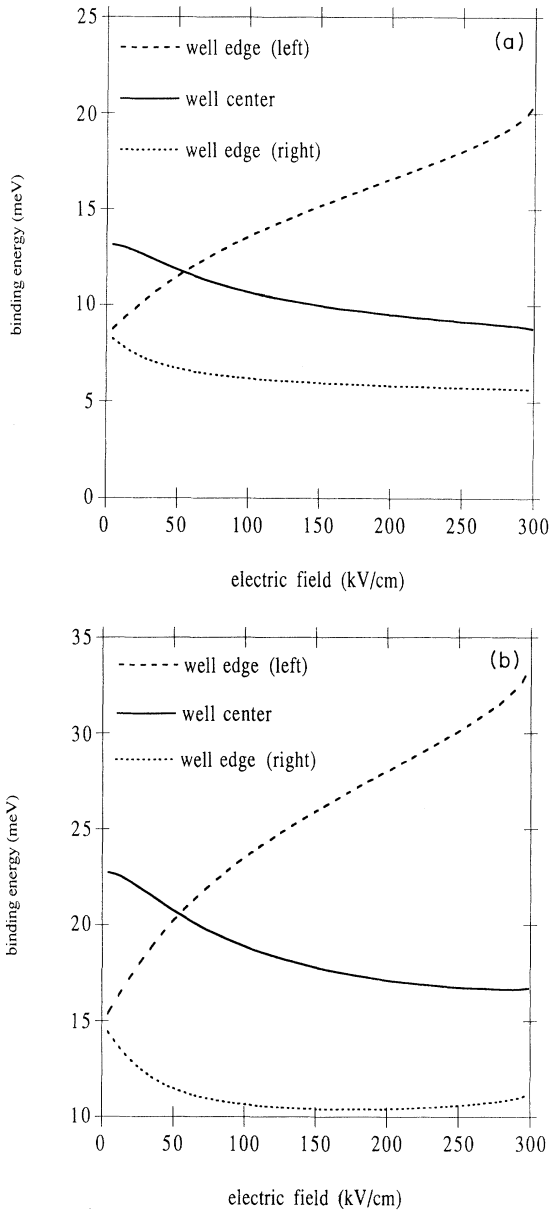

FIG. 6. Variation of the $1s$ donor binding energy as a function of the electric field, in a 200-Å GaAs-ZnSe dielectric quantum well for donors located at the center and at the edges of the quantum well, (a) in zero magnetic field, (b) in a 200-kG magnetic field.

binding energies become smaller than those in curve 1.

In Figs. 3(a) and 3(b), we show the variation of the $1s$ binding energy and that of the $1s \rightarrow 2p_+$ transition energy of a donor located (a) at the center and (b) at the edge of a GaAs-ZnSe dielectric QW, as a function of the quantum-well size, in various magnetic fields. For the well sizes shown here, both the $1s$ binding energy and the $1s \rightarrow 2p_+$ transition energy are monotonic functions of the QW size. At small sizes, they should approach the corresponding values in the bulk ZnSe, which are substantially higher than those in GaAs, so whether a maximum appears in the $1s$ binding energy or the $1s \rightarrow 2p_+$ transition energy in the case of dielectric QW's cannot be as definite as in the case of ordinary QW's.

In Fig. 4, we display the variations of the binding energies of the $1s$ state and the $1s \rightarrow 2p_+$ transition energies in a dielectric quantum well as functions of the applied magnetic field, in the absence of the electric field. Two cases are considered (i) a donor located at the center, and (ii) a donor at the edges of a 100-Å-wide quantum well. Because the electron wave function is concentrated in the middle of the quantum well, binding energies of the $1s$ and $2p$ states of the center donor are higher than those of the edge donor. The same is true for the $1s \rightarrow 2p_+$ transition energies. Since the magnetic field provides an additional confinement in the transverse directions, both the binding energies and the $1s \rightarrow 2p_+$ transition energies increase as functions of the magnetic field.

In Fig. 5, we compare the $1s$ binding energy and the $1s \rightarrow 2p_+$ transition energy in a dielectric QW in the absence of the electric field, with those in the presence of a 200-kV/cm electric field. As expected, for small QW sizes (≤ 50 Å here), the values of the $1s$ binding energy and the $1s \rightarrow 2p_+$ transition are not affected by the presence of the electric field. The electron wave function is significantly modified by the applied electric field only at larger QW sizes, leading to smaller values of the $1s$ binding energy and the $1s \rightarrow 2p_+$ transition energy for a donor located at the center of the QW.

To see how the electric field affects the $1s$ binding energy and the $1s \rightarrow 2p_+$ transition energy of a donor located at the edges and at the center of a dielectric QW, we plot in Figs. 6(a) and 6(b) the $1s$ binding energy and the $1s \rightarrow 2p_+$ transition energy as a function of the electric field, in a 200-Å QW in (a) a zero magnetic field and (b) a 200-kG magnetic field. Since the electron wave function is mostly inside the quantum well in the absence of the electric field, it is clear that the different behaviors exhibited by donors at different locations are caused by the electron wave function being modified in the QW structure. As the electric field is increased, the electron is pulled toward one side of the QW. As a result, the binding energies decrease as a function of the electric field for the donor located at the part of the QW where the probability of finding the electron is reduced (the center and the right edge in this case), and increase for the donor located at the part where such a probability is increased. Such behavior is also found for a donor in an ordinary QW. Although the image charge distribution contributes to the quantitative enhancement of the binding energies in the dielectric QW, it apparently does not lead to significant qualitative differences.

SUMMARY

In conclusion, we have developed a formalism for studying the energy levels of confined donor states in a dielectric quantum-well structure in the presence of parallel electric and magnetic fields applied along the growth direction, and have calculated binding energies of the $1s$ state and the $1s \rightarrow 2p_+$ transition energies associated with the lowest electronic subband. The effect of the ratio of the two dielectric constants on the donor binding energies is also discussed. The additional confinement due to the image charge distribution is shown to significantly enhance the binding energies and the $1s \rightarrow 2p_+$ transition energies of donor states in the dielectric quantum-well structures. It is also shown that although the image charge distribution contributes to the quantitative enhancement of the binding energies in the dielectric QW, it apparently does not lead to significant qualitative differences. In addition, it is also shown that for QW sizes often encountered in experiments, the effect of the dielectric confinement on the energy levels can be accounted for to within a few meV's in a simplified formalism by using the average dielectric constant throughout the QW structure. Experimental efforts are encouraged to lend support to our calculations.

ACKNOWLEDGMENTS

This work was supported by the Air Force Office of Scientific Research under Grants Nos. AFOSR-91-0056 and AFOSR-90-0118.

[1]L. V. Keldysh, Pis'ma Zh. Eksp. Teor. Fiz. **29**, 716 (1979) [JETP Lett. **29**, 658 (1979)].
[2]L. V. Keldysh, Superlatt. Microstruct. **4**, 637 (1988).
[3]M. Kumagai and T. Takagahara, Phys. Rev. B **40**, 12 359 (1989), and references therein.
[4]D. B. Tran Thoai, R. Zimmermann, M. Grundmann, and D. Bimberg, Phys. Rev. B **42**, 5906 (1990).
[5]X. Hong, T. Ishihara, and A. V. Nurmikko, Phys. Rev. B **45**, 6961 (1992).
[6]S. Zhang and N. Kobayashi, Appl. Phys. Lett. **60**, 883 (1992).
[7]K. J. Han, A. Abbate, I. B. Bhat, and P. Das, Appl. Phys. Lett. **60**, 862 (1992).
[8]T. Ishihara, Jun Takahashi, and T. Goto, Phys. Rev. B **42**, 11 099 (1990).
[9]L. Bányai, I. Galbraith, C. Ell, and H. Haug, Phys. Rev. B **36**, 6099 (1987).
[10]T. Ogawa and T. Takagahara, Phys. Rev. B **44**, 8138 (1991).
[11]G. Bastard, Phys. Rev. B **24**, 4714 (1981).
[12]C. Mailhiot, Y.-C. Chang, and T. C. McGill, Phys. Rev. B **26**, 4449 (1982).
[13]R. L. Greene and K. K. Bajaj, Solid State Commun. **45**, 825 (1983).

[14]S. Chaudhuri, Phys. Rev. B **28**, 4480 (1983).
[15]K. Tanaka, M. Nagaoka, and T. Yamabe, Phys. Rev. B **28**, 7068 (1983).
[16]W. T. Masselink, Y. C. Chang, and H. Morkoç, Phys. Rev. B **28**, 7373 (1983).
[17]S. Chaudhuri and K. K. Bajaj, Phys. Rev. B **29**, 1803 (1984).
[18]C. Priester, G. Bastard, G. Allan, and M. Lannoo, Phys. Rev. B **30**, 6029 (1984).
[19]J. A. Brum, C. Priester, and G. Allan, Phys. Rev. B **32**, 2378 (1985).
[20]Ronald L. Greene and K. K. Bajaj, Solid State Commun. **53**, 1103 (1985); Phys. Rev. B **31**, 913 (1985).
[21]W. Liu and J. J. Quinn, Phys. Rev. B **31**, 2348 (1985).
[22]N. C. Jarosik, B. D. McCombe, B. V. Shanabrook, J. Comas, J. Ralston, and G. Wicks, Phys. Rev. Lett. **54**, 1283 (1985).
[23]P. Lane and R. L. Greene, Phys. Rev. B **33**, 5871 (1986); R. L. Greene and P. Lane, *ibid.* **34**, 8639 (1986).
[24]Ronald L. Greene and K. K. Bajaj, Phys. Rev. B **34**, 951 (1986).
[25]M. Stopa and S. Das Sarma, Phys. Rev. B **40**, 8466 (1989).
[26]J. P. Cheng and B. D. McCombe, Phys. Rev. B **42**, 7626 (1990).
[27]C.-M. Dai and D.-S. Chuu, Physica B **172**, 445 (1991).
[28]K. F. Ilaiwi and M. Tomak, Phys. Rev. B **42**, 3132 (1990).
[29]S. I. Tsonchev and P. L. Goodfriend, Phys. Rev. B **44**, 1329 (1991).
[30]J. M. Shi, F. M. Peeters, G. Q. Hai, and J. T. Devreese, Phys. Rev. B **44**, 5692 (1991).
[31]Byungsu Yoo, B. D. McCombe, and W. Schaff, Phys. Rev. B **44**, 13 152 (1991).
[32]R. Ranganathan, B. D. McCombe, N. Nguyen, Y. Zhang, M. L. Rustgi, and W. J. Schaff, Phys. Rev. B **44**, 1423 (1991).
[33]J. Cen and K. K. Bajaj, Phys. Rev. B **46**, 15 280 (1992).
[34]W. K. H. Panofsky and M. Phillips, *Classical Electricity and Magnetism,* 2nd ed. (Addison-Wesley, New York, 1962), pp. 89 and 90.
[35]J. Cen, S. M. Lee, and K. K. Bajaj, J. Appl. Phys. **73**, 2848 (1993).
[36]J. Cen and K. K. Bajaj (unpublished).
[37]J. Cen, S. V. Branis, and K. K. Bajaj, Phys. Rev. B **44**, 12 848 (1991).
[38]G. Bastard, E. E. Mendez, L. L. Chang, and L. Esaki, Phys. Rev. B **28**, 3241 (1983).
[39]S. Huzinaga, J. Chem. Phys. **42**, 1293 (1965).